

**Link sito dell'editore:** <https://arc.aiaa.org/doi/10.2514/1.G002182>

**Link codice DOI:** 10.2514/1.G002182

**Citazione bibliografica dell'articolo:**

Alessandro Zavoli, Guido De Matteis, Fabrizio Giuliotti, Giulio Avanzini, "Single-Axis pointing of an underactuated spacecraft equipped with two reaction wheels", *Journal of Guidance, Control, and Dynamics*, Vol. 40, No. 6, Giu. 2017, pp. 1465-1471

# Single axis pointing of an underactuated spacecraft equipped with two reaction wheels

A. Zavoli<sup>1</sup> and Guido De Matteis<sup>2</sup>  
*'Sapienza' Università di Roma, Rome, 00184, Italy*

F. Giulietti<sup>3</sup>  
*Università di Bologna (Forlì Campus), Forlì, 47121, Italy*

G. Avanzini<sup>4</sup>  
*Università del Salento, Lecce, 73100, Italy*

## I. Introduction

The note proposes a novel approach for single-axis pointing of an underactuated spacecraft using only two reaction wheels (RW), based on a simple yet effective wheel rate command. The control law can be used for aiming the line-of-sight of a sensor, a nozzle or an antenna towards a target direction, or solar panels towards the Sun, after failure of one wheel for a non-redundant control system hardware or in the case of multiple failures for redundant systems. Examples of this kind of situation are the Far Ultraviolet Spectroscopic Explorer (FUSE) [1] and the Kepler space telescope [2, 3]. Both spacecraft suffered from failures that left only two wheels available for maneuvers. Failure of mechanical actuators is also expected to potentially affect low-budget space missions based on small-size low-cost spacecraft (nano-, pico-, and cube-sat families).

The proposed control methodology represents the practical, dynamic implementation of the kinematic planning scheme discussed in [4], under the assumptions of zero overall angular momentum and triaxial inertia tensor. Under the zero-angular momentum hypothesis, the control law also

---

<sup>1</sup> Research Assistant, Department of Mechanical and Aerospace Engineering, Via Eudossiana 18, AIAA Member.

<sup>2</sup> Professor, Department of Mechanical and Aerospace Engineering, Via Eudossiana 18, AIAA Member.

<sup>3</sup> Associate Professor, Department of Industrial Engineering (DIN), Via Fontanelle 40, AIAA Senior Member.

<sup>4</sup> Professor, Department of Engineering, Campus Ecotekne (Corpo O), Via per Monteroni, AIAA Senior Member.

provides three-axis stabilization at zero angular speed. Only rest-to-rest maneuvers are thus dealt with, as a steady residual rotation rate around an arbitrary body-fixed axis cannot be attained in general, unless the axis is principal of inertia and aligned with the spin axis of one of the two active reaction wheels. The limited computational demand of the control law makes it a practical solution also in the case of small-size satellites, where the computational budget is severely limited by the available CPU processing capabilities. The effects of a non-zero residual angular momentum and control axes not aligned with the principal axes of inertia is also investigated, highlighting limitations on pointing precision and convergence performance.

The problem of spacecraft attitude control with two control torques is a relevant topic in the literature. Tsiotras and Longuski [5] presented a methodology for constructing feedback laws for attitude stabilization about the symmetry axis. Kim and Kim [6] also considered the problem of spin stabilization of a spacecraft using two reaction wheels, exploiting the  $z$ - $w$  parametrization introduced by Tsiotras *et al.* [7] to derive a control law that globally asymptotically stabilizes the spacecraft on a revolving motion around a specified inertial axis. A time-variant discontinuous singular controller was proposed by Horri *et al.* for 3-axis attitude stabilization of a satellite with zero angular momentum, when attitude is described by either Rodrigues parameters [8] or quaternions [9]. Yoon and Tsiotras [10] considered a spacecraft equipped with a single VSCMG, deriving a linear quadratic regulator (LQR) to locally stabilize spacecraft angular rate, while controlling the direction of a given body-fixed axis in the inertial space. A multi-stage control law was suggested to attain global convergence.

Avanzini and Giulietti [4] proposed a kinematic planning scheme for eigenaxis rotations that allows for aiming a body-fixed axis  $\hat{\sigma}$  towards a prescribed direction  $\hat{\tau}$ , in the presence of constraints on the admissible rotation axis, when there is a direction  $\hat{b}$  around which a control torque component is not available and angular velocity commands are thus constrained on a plane perpendicular to  $\hat{b}$ . The technique was recently extended [11] in order to determine a sequence of feasible rotations with minimum total angular path, to be applied when the axis  $\hat{\sigma}$  is also required to stay away from inadmissible directions, such as bright radiation sources that may harm sensor hardware.

In Refs. [4] and [11] the (sequence of) admissible rotation(s) is identified in terms of eigenaxis

$\hat{\mathbf{g}}_\Gamma$ , perpendicular to  $\hat{\mathbf{b}}$ , and rotation amplitude  $\hat{\alpha}$ , in the framework of magnetic control, where magnetic torquers are used as attitude effectors and the torqueless direction  $\hat{\mathbf{b}}$  is represented by the geomagnetic field, prescribed in the orbit frame. Magnetic actuation results into an inherently underactuated system, which severely limits its practical use. Nonetheless, an underactuated condition may also be the consequence of mechanical hardware failure, in which case the same planning scheme can still be adopted, when a spacecraft is equipped with only two operational reaction wheels and the torqueless direction  $\hat{\mathbf{b}}$  is prescribed in the body frame.

In this note, a smooth time-invariant wheel rate command is defined, based on angular momentum balance considerations, which causes the spacecraft to rotate approximately about the admissible rotation axis  $\hat{\mathbf{g}}_\Gamma$ , lying on the plane identified by the two RW axes, thus implementing the kinematic planning scheme of Ref. [4] at a dynamic level. Convergence towards the prescribed alignment under the action of the proposed control law is proven using a Lyapunov approach, exploiting the cascade (triangular) nature of system dynamics. Asymptotic convergence in a finite region around the desired final condition is proven first. Almost global attractiveness is then verified over the entire phase-space, excluding a single unstable equilibrium point. As a further contribution, a modified version of the control law is also discussed, featuring a switching control logic, with the objective of improving convergence speed. In this case control performance is assessed through simulations. A stability proof is no longer pursued, because discontinuities introduced in the system pose formal issues when using Lyapunov theory.

In the next Section, the satellite model is outlined and the main features of the kinematic planning scheme are recalled. In Section III, the nominal control law is presented first, together with a rigorous proof of its stability for the ideal case of zero-angular momentum. A modified version of the control law is then introduced. In Section IV, performance of the two control laws is investigated by means of numerical simulations. A Section of concluding remarks ends the note.

## II. Problem statement and solution

### A. Mathematical model

A satellite platform equipped with three identical reaction wheels is considered. Expressing all vector quantities in a set of body-fixed axes,  $\mathbb{F}_B = \{G, \hat{e}_1, \hat{e}_2, \hat{e}_3\}$  centered in the spacecraft center of mass  $G$ , spacecraft attitude dynamics is described by the following equations of motion

$$\dot{\mathbf{T}}_{BN} = -\mathbf{\Omega}^\times \mathbf{T}_{BN} \quad (1)$$

$$\dot{\boldsymbol{\omega}} = \mathbf{J}^{-1} \left[ -\boldsymbol{\omega} \times (\mathbf{J}\boldsymbol{\omega} + \mathbf{h}_w) - \dot{\mathbf{h}}_w \right] \quad (2)$$

$$\dot{h}_{w,i} = J_w \dot{\Omega}_i = g_i - J_w \dot{\boldsymbol{\omega}}^T \hat{\mathbf{a}}_i, \quad i = 1, 2, 3 \quad (3)$$

where  $\mathbf{T}_{BN}$  is the transformation matrix from inertial to body reference frame,  $\boldsymbol{\omega} = (\omega_1, \omega_2, \omega_3)^T$  is the inertial angular velocity vector,  $\mathbf{\Omega}^\times$  is the cross-product equivalent matrix, such that  $\mathbf{\Omega}^\times \mathbf{v} = \boldsymbol{\omega} \times \mathbf{v}$ ,  $h_{w,i} = J_w \Omega_i$  is the relative angular momentum vector of the  $i$ -th reaction wheel, spinning at a relative angular rate  $\Omega_i$  around the control axis  $\hat{\mathbf{a}}_i$ , under the action of an electrical motor torque  $g_i$ , and  $\mathbf{J}$  is the satellite inertia matrix (which includes wheel inertia at rest). The vector  $\mathbf{h}_w = \sum_{i=1}^3 J_w \Omega_i \hat{\mathbf{a}}_i$  is the total internal angular momentum. It is assumed that principal axes of inertia are parallel to wheel spin axes,  $\hat{\mathbf{e}}_i = \hat{\mathbf{a}}_i$ ,  $i = 1, 2, 3$ . Without loss of generality, it is assumed that the underactuated axis is  $\hat{\mathbf{b}} = \hat{\mathbf{e}}_3$ . As a consequence, only two RW's are available, with spin axes parallel to  $\hat{\mathbf{e}}_1$  and  $\hat{\mathbf{e}}_2$ , respectively.

When represented in  $\mathbb{F}_B$ , the unit vectors  $\hat{\mathbf{b}}$  (the underactuated direction) and  $\hat{\boldsymbol{\sigma}}$  (the axis that needs to be pointed towards a prescribed direction) are both constant. At the same time the angular position of the spacecraft about  $\hat{\boldsymbol{\sigma}}$  is not relevant, as far as the single-axis-pointing problem is concerned. Consequently, problem kinematics can be simplified by focusing on the analysis of the motion of the inertially fixed target unit vector  $\hat{\boldsymbol{\tau}}$  with respect to  $\mathbb{F}_B$ , so that Eq. (1) is substituted by the time derivative of  $\hat{\boldsymbol{\tau}}$  expressed in the body-fixed frame

$$\dot{\hat{\boldsymbol{\tau}}} = -\boldsymbol{\omega} \times \hat{\boldsymbol{\tau}} \quad (4)$$

Under the assumption of zero initial angular momentum and neglecting external torques, the total angular momentum  $\mathbf{h} = \mathbf{J}\boldsymbol{\omega} + \mathbf{h}_w$  remains constantly zero. A vector  $\mathbf{u} = (u_1, u_2, u_3)^T$  of

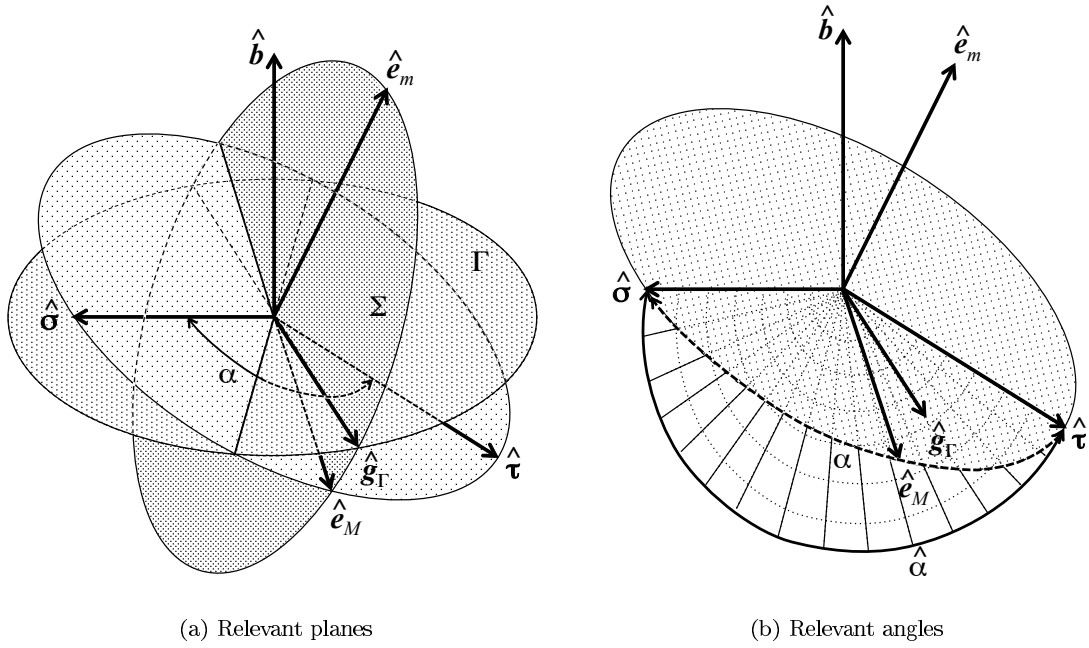


**Figure 1** Geometry of the problem and notation for the planning scheme.

virtual controls  $u_i = -(g_i - J_w \dot{\omega}^T \hat{a}_i)$  can be introduced, so that Eqs. (2) and (3) reduce to

$$J\dot{\omega} = u \quad (5)$$

$$\dot{h}_w = -u \quad (6)$$

In the absence of an active reaction wheel spinning around  $\hat{b} = \hat{e}_3$ , the third component of the angular velocity vector  $\omega_3$  remains identically zero throughout the maneuver and  $h_w \equiv -J\omega$ .

## B. Kinematic planning scheme

Following concepts and notation introduced in [4], a body-fixed axis  $\hat{\sigma}$  need to be aligned with a desired direction  $\hat{\tau}$ , starting from an initial condition such that  $\hat{\sigma} \cdot \hat{\tau} = \cos \alpha$ . The desired alignment can be obtained by means of an eigenaxis rotation of amplitude  $\hat{\alpha}$  around an axis  $\hat{g}$  that belongs to the plane  $\Sigma$  defined by the unit vectors  $\hat{e}_m = (\hat{\sigma} \times \hat{\tau}) / \|\hat{\sigma} \times \hat{\tau}\|$  and  $\hat{e}_M = (\hat{\sigma} + \hat{\tau}) / \|\hat{\sigma} + \hat{\tau}\|$  (Fig. 1.a), which identify the rotation axes of minimum ( $\hat{\alpha} = \alpha$ ) and maximum ( $\hat{\alpha} = \pi$ ) angular travel, respectively. In order to allow for an admissible rotation, the eigenaxis must also belong to the plane  $\Gamma$ , perpendicular to  $\hat{b}$ , identified in the proposed scenario by the plane containing the spin axes of the two active RW's. Under the assumption of zero total angular momentum, both RW torque and spacecraft angular speed are constrained on the plane  $\Gamma$ . The error vector  $\varepsilon_1 = \hat{\tau} - \hat{\sigma}$  is

perpendicular to the plane  $\Sigma$ , whereas the underactuated direction  $\hat{\mathbf{b}}$  is normal to the plane  $\Gamma$  that contains the admissible rotation axes. The admissible rotation axis is thus identified by the unit vector

$$\hat{\mathbf{g}}_\Gamma = \frac{(\hat{\boldsymbol{\tau}} - \hat{\boldsymbol{\sigma}}) \times \hat{\mathbf{b}}}{\|(\hat{\boldsymbol{\tau}} - \hat{\boldsymbol{\sigma}}) \times \hat{\mathbf{b}}\|} \quad (7)$$

which lies at the intersection of  $\Gamma$  and  $\Sigma$ . During the motion,  $\hat{\boldsymbol{\sigma}}$  spans a portion of amplitude  $\hat{\alpha}$  of the cone with axis equal to  $\hat{\mathbf{g}}_\Gamma$  (Fig. 1.b). The idea at the basis of the present note is to derive an angular rate command for the active wheels that results into a rotation of the spacecraft (almost exactly) around the admissible rotation eigenaxis  $\hat{\mathbf{g}}_\Gamma$ .

### III. Control law and proof of stability

The dynamic system of Eqs. (4)-(5) exhibits a triangular (or cascade) structure, where the angular speed  $\boldsymbol{\omega}$  acts as a virtual input for the kinematics (outer system), whereas the virtual control  $\mathbf{u}$  represents the input torque to spacecraft dynamics (inner system). It is apparent that any angular speed command can be tracked, provided that it has a zero component along the direction of the failed axis,  $\hat{\mathbf{b}}$ , and it does not violate wheel rate saturation limits. In this respect, a desired angular speed profile  $\boldsymbol{\omega}_d$  is sought first, which stabilizes the outer system. Next, a virtual torque command  $\mathbf{u} = \mathbf{u}(\boldsymbol{\omega}_d)$  is derived for the inner angular rate control.

The proposed control law is defined by the following equations

$$\boldsymbol{\omega}_d = -k_\tau(\hat{\boldsymbol{\tau}} - \hat{\boldsymbol{\sigma}}) \times \hat{\mathbf{b}} \quad (8a)$$

$$\mathbf{u} = \mathbf{J}[\dot{\boldsymbol{\omega}}_d + k_\omega(\boldsymbol{\omega}_d - \boldsymbol{\omega})] \quad (8b)$$

where  $k_\tau$  and  $k_\omega$  are positive gains.

Before deriving a rigorous proof of stability for the interconnected system, the properties of the outer kinematic system are discussed, assuming that the angular velocity exactly matches  $\boldsymbol{\omega}_d$ . In this case, upon substitution of Eq. (8a) into Eq. (4), the kinematic equation takes the form

$$\dot{\hat{\boldsymbol{\tau}}} = -k_\tau \hat{\boldsymbol{\tau}} \times [(\hat{\boldsymbol{\tau}} - \hat{\boldsymbol{\sigma}}) \times \hat{\mathbf{b}}] \quad (9)$$

Note that the phase-space for the kinematic system is the compact two-dimensional set  $\mathcal{S}^2 \subset \mathbb{R}^3$ , representing the surface of a unit sphere in a three-dimensional Cartesian space, defined by the

axes of the body-frame  $\mathcal{F}_B$ . The position of  $\hat{\tau}$  on  $\mathcal{S}^2$  can be identified by means of two spherical coordinates,  $\varphi$  and  $\lambda$ . Without loss of generality,  $\hat{\mathbf{b}}$  is chosen as polar axis of  $\mathcal{S}^2$ . The equatorial plane,  $\lambda = 0$ , coincides with the plane of admissible rotation axes. The prime meridian,  $\varphi = 0$ , is chosen so that  $\hat{\sigma}$  (fixed with respect to  $\mathcal{F}_B$ ) lies on it. The position of  $\hat{\sigma}$  is identified by its latitude,  $\lambda_\sigma$ , which states its elevation above the plane of the two active RWs,  $\hat{\mathbf{e}}_1$  and  $\hat{\mathbf{e}}_2$ .

The dynamic system in Eq. (9) admits two fixed points in  $\mathcal{S}^2$ , namely  $P$  and  $P_\#$ . The first equilibrium corresponds to the desired alignment,  $\hat{\tau} = \hat{\sigma}$ , whereas the second non-trivial, undesired, equilibrium is such that  $\hat{\tau} - \hat{\sigma} \parallel \hat{\mathbf{b}}$ . The latter case requires that the unit vectors  $\hat{\mathbf{b}}$ ,  $\hat{\tau}$ , and  $\hat{\sigma}$  lie on the same plane, with  $\hat{\tau} = \hat{\sigma}_\#$ , where  $\hat{\sigma}_\# \equiv \hat{\sigma} - 2(\hat{\mathbf{b}}^T \hat{\sigma}) \hat{\mathbf{b}}$ . Figure 2 shows the vector field of  $\dot{\hat{\tau}}$  resulting from Eq. (9), for an assigned direction  $\hat{\sigma}$ , to qualitatively highlight the stability of the two equilibria. The equilibrium above the equator is clearly stable, whereas the other one is unstable. Thus, when  $\hat{\sigma}^T \hat{\mathbf{b}} > 0$ , (i.e.,  $\hat{\sigma}$  belongs to the Northern hemisphere), the stable equilibrium corresponds to the desired alignment, whereas the undesired equilibrium is unstable. When  $\hat{\sigma}^T \hat{\mathbf{b}} < 0$  the two equilibrium points switch their positions. Provided that the sense of the failed axis  $\hat{\mathbf{b}}$  is arbitrary, the direction of the vector can be reversed to obtain the case with  $\hat{\mathbf{b}}^T \hat{\sigma} > 0$ . As a limit case, when  $\hat{\sigma}^T \hat{\mathbf{b}} = 0$  the two equilibria merge on a point on the equator of  $\mathcal{S}^2$ , which is still globally attractive, although it is no longer stable in the sense of Lyapunov.

### A. Proof of stability

The proof of stability of the proposed control law, Eq. (8), is obtained by application of a theorem taken from Ref. [12] (see Corollary 4.3), which provides sufficient conditions for global asymptotic stability (GAS) of a triangular system.

**Theorem 1** *Consider the dynamic triangular system*

$$\dot{\mathbf{x}} = \mathbf{f}(\mathbf{x}, \mathbf{y}) \tag{10a}$$

$$\dot{\mathbf{y}} = \mathbf{g}(\mathbf{y}) \tag{10b}$$

*If A1)  $\mathbf{y} = 0$  is GAS for (10a), A2)  $\mathbf{x} = 0$  is GAS for  $\dot{\mathbf{x}} = \mathbf{f}(\mathbf{x}, \mathbf{0})$ , and A3) every solution of (10a) is bounded for  $t > 0$ , then the system (10) is GAS.*



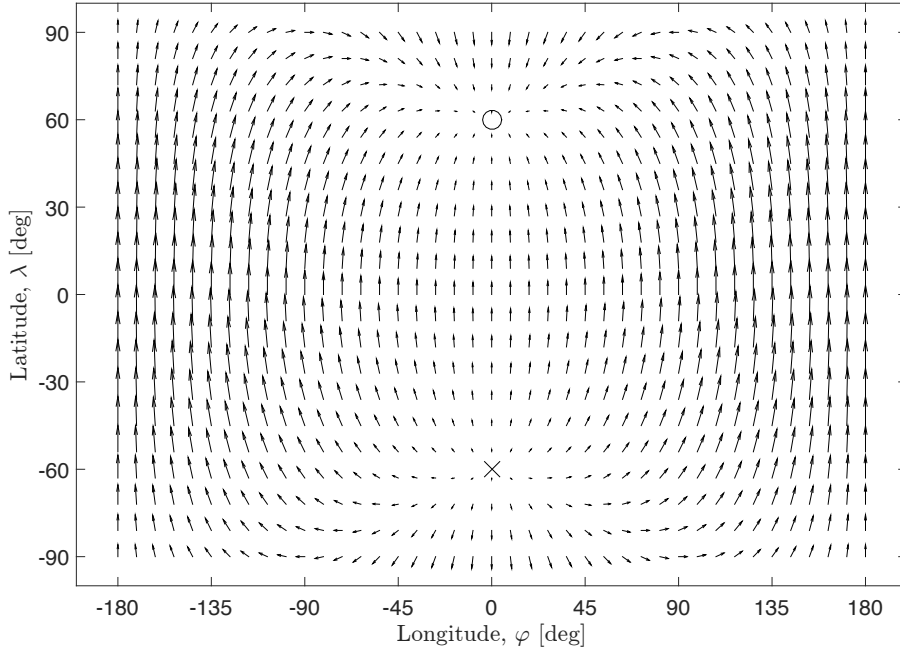


**Figure 2** Velocity of  $\hat{\tau}$  on the unit sphere  $S^2$  for the ideal case,  $\omega \equiv \omega_d$ ,  $\lambda_\sigma = 60^\circ$ ; equilibria  $P$  and  $P_\#$  are indicated by circle (o) and cross marks (x), respectively.

First of all, two error variables are introduced, namely  $\varepsilon_1 = \hat{\tau} - \hat{\sigma}$  and  $\varepsilon_2 = \omega_d - \omega$ , for pointing direction and angular rate, respectively. By taking into account the control law proposed in Eq. (8), the dynamic system given by Eqs. (4)-(5) can be recast in error form as

$$\dot{\varepsilon}_1 = k_\tau (\varepsilon_1 \times \mathbf{b}) \times (\boldsymbol{\sigma} + \varepsilon_1) + \varepsilon_2 \times (\boldsymbol{\sigma} + \varepsilon_1) \quad (11a)$$

$$\dot{\varepsilon}_2 = -k_\omega \varepsilon_2 \quad (11b)$$

which clearly matches the form of Theorem 1. Almost global asymptotic stability of the controller is proven, showing that all assumptions of Theorem 1 hold. Assumption A1 is easily verified, provided that Eq. (11b) represents a first-order stable dynamics for the angular rate error.

In order to verify assumption A2, one needs to prove that  $\varepsilon_1 = \mathbf{0}$  is GAS for the system

$$\dot{\varepsilon}_1 = k_\tau (\varepsilon_1 \times \hat{\mathbf{b}}) \times (\hat{\boldsymbol{\sigma}} + \varepsilon_1) \quad (12)$$

This is equivalent to the analysis of the stability for the equilibrium  $P$  of Eq. (9). Asymptotic stability of the equilibrium  $P$  under the control law Eq. (8a) over a finite region  $\mathcal{A} \subseteq S^2$  can be assessed considering the Lyapunov candidate function  $V_1 = 1 - (\hat{\boldsymbol{\sigma}}^T \hat{\boldsymbol{\tau}}) = 1 - \cos \alpha$ , where  $\alpha$  is the angular separation between  $\hat{\boldsymbol{\sigma}}$  and  $\hat{\boldsymbol{\tau}}$ , The function  $V_1$  is clearly positive definite and proper. The

time derivative of  $V_1$  is given by

$$\dot{V}_1 = -k_\tau \left(1 - \hat{\sigma}^T \hat{\tau}\right) \left(\hat{\tau}^T \hat{\mathbf{b}} + \hat{\sigma}^T \hat{\mathbf{b}}\right) \quad (13)$$

Clearly  $\dot{V}_1 \leq 0$  it is negative valued in  $\mathcal{A} = \left\{\hat{\tau} \in \mathcal{S}^2 : \hat{\mathbf{b}}^T \hat{\tau} + \hat{\mathbf{b}}^T \hat{\sigma} > 0\right\}$ . The region  $\mathcal{A}$  extends to the section of  $\mathcal{S}^2$  to the north of the parallel passing by  $\hat{\sigma}_\#$ . Inside  $\mathcal{A}$ ,  $\dot{V}_1$  is null only for  $\hat{\tau} = \hat{\sigma}$ , that is, when  $\varepsilon_1 = 0$ . The equilibrium point  $P$  is thus asymptotically stable, with a domain of attraction at least as large as the subset  $\mathcal{A}$  of  $\mathcal{S}^2$ .

Analogously, one can prove that, assuming  $\hat{\mathbf{b}}^T \hat{\sigma} > 0$ , the equilibrium  $P_\#$  is unstable under the control law Eq. (8a). A ‘‘domain of divergence’’ can be determined using Lyapunov’s First Instability Theorem (see [13], Theorem 3.12). If one considers the function  $V_2 = 1 - \left(\hat{\sigma}_\#^T \hat{\tau}\right) = 1 - \cos \alpha_\#$ , such that  $V(\hat{\sigma}_\#) = 0$ , and  $V(\hat{\tau}) > 0$  for  $\hat{\tau} \neq \hat{\sigma}_\#$ , its time derivative is given by

$$\dot{V}_2 = -k_\tau \left(\hat{\mathbf{b}}^T \hat{\tau} - \hat{\mathbf{b}}^T \hat{\sigma}\right) \left(1 - \hat{\tau}^T \hat{\sigma}_\#\right) \quad (14)$$

It is easy to prove that  $\dot{V}_2 > 0$ , that is, the angular separation  $\alpha_\#$  between  $\hat{\tau}$  and  $\hat{\sigma}_\#$  increases over time when  $\hat{\tau} \in \mathcal{A}^\# = \left\{\hat{\tau} \in \mathcal{S}^2 : \hat{\mathbf{b}}^T \hat{\tau} - \hat{\mathbf{b}}^T \hat{\sigma} < 0\right\} \setminus \{\hat{\sigma}_\#\}$ . For the sake of clarity, Fig. 3 illustrates the regions  $\mathcal{A}$  and  $\mathcal{A}_\#$  in the plane  $\lambda - \varphi$ . As a consequence of the instability of  $P_\#$ , all solutions starting in the region  $\mathcal{A}_\#$  at a finite distance from  $\hat{\sigma}_\#$  leave the set  $\mathcal{A}_\#$  in a finite time. Moreover, if  $\hat{\sigma}^T \hat{\mathbf{b}} > 0$ , then  $\mathcal{A}_\# \cap \mathcal{A} \neq \emptyset$ , that is, the region of divergence surrounding  $P_\#$  and the domain of attraction of  $P$  overlap. As a result,  $P$  is almost GAS, provided that its domain of attraction extends to  $\mathcal{S}^2 \setminus \{P_\#\}$ . Assumption A2 is thus verified almost everywhere over  $\mathcal{S}^2$ .

Finally, it is necessary to prove that all the solutions of the interconnected system Eqs. (11) are bounded. The error variable  $\varepsilon_1$  is the difference between two unit vectors, thus  $\|\varepsilon_1\| \leq 2$ . On the other hand,  $\|\varepsilon_2(t)\| \leq \|\varepsilon_2(t_0)\|$  because Eq. (11b) enforces a first-order stable dynamics. Recalling the definition of  $\varepsilon_2$  and boundness of  $\varepsilon_1$ , the chain of inequalities

$$\begin{aligned} \|\varepsilon_2(t)\| &\leq \|\varepsilon_2(t_0)\| = \|\boldsymbol{\omega}(t_0) - \boldsymbol{\omega}_d(t_0)\| \\ &\leq \|\boldsymbol{\omega}(t_0)\| + \|\boldsymbol{\omega}_d(t_0)\| = \|\boldsymbol{\omega}(t_0)\| + \|k_\tau \varepsilon_1(t_0) \times \hat{\mathbf{b}}\| \leq \|\boldsymbol{\omega}(t_0)\| + 2k_\tau \end{aligned}$$

demonstrates that also assumption A3 holds. Therefore all hypotheses of Theorem 1 are satisfied, and the origin of the cascade system  $(\varepsilon_1, \varepsilon_2) = \mathbf{0}$  is almost globally asymptotically stable over  $\mathcal{S}^2$ .

The case  $\hat{\sigma}^T \hat{\mathbf{b}} = 0$  deserves a specific discussion. As  $|\hat{\sigma}^T \hat{\mathbf{b}}| \rightarrow 0$ , the unit vectors  $\hat{\sigma}$  and  $\hat{\sigma}_\#$  move towards the equator of  $\mathcal{S}^2$ , the sets  $\mathcal{A}$  and  $\mathcal{A}_\#$  shrink, and their overlapping region reduces. In the limit circumstance of  $\hat{\sigma}^T \hat{\mathbf{b}} = 0$ ,  $\hat{\sigma}$  and  $\hat{\sigma}_\#$  coincide, the system Eq. (12) admits only one equilibrium point on the equator, and the two sets  $\mathcal{A}$  and  $\mathcal{A}_\#$  reduce to the Northern and Southern hemisphere of  $\mathcal{S}^2$ , respectively. Both  $\dot{V}_1$  and  $\dot{V}_2$  vanish on the equator of  $\mathcal{S}^2$ ,  $\mathcal{E} \equiv \partial\mathcal{A} = \partial\mathcal{A}_\#$ , but the angular velocity command is non-zero everywhere except for  $\hat{\tau} = \hat{\sigma}$ . More precisely, the time derivative for  $\hat{\tau} \in \mathcal{E}$ , obtained from Eq. (9) for  $\hat{\tau}^T \hat{\mathbf{b}} = 0$ , is  $\dot{\hat{\tau}} = k_\tau [\hat{\tau}^T (\hat{\tau} - \hat{\sigma})] \hat{\mathbf{b}}$ , that is, parallel to  $\hat{\mathbf{b}}$  and traversal to  $\mathcal{E}$ . Provided that no trajectory lies on  $\mathcal{E} \setminus \{\hat{\sigma}\}$ , La Salle invariance principle guarantees that  $\hat{\tau} = \hat{\sigma}$  is still globally attractive, although no longer stable in the sense of Lyapunov.

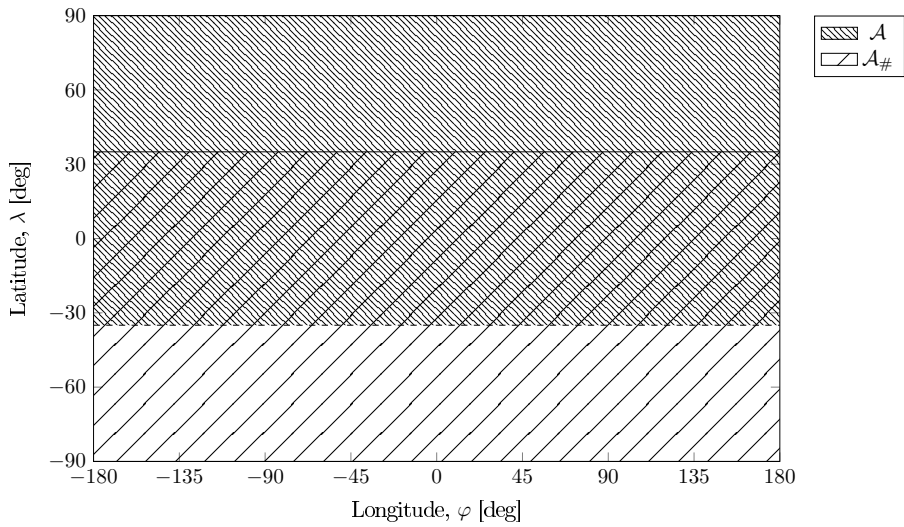


**Figure 3** Sketch of regions  $\mathcal{A}$  (domain of attraction of stable equilibrium point  $P$ ) and  $\mathcal{A}_\#$  (domain of divergence for the unstable equilibrium  $P_\#$ ).

### B. Modified control law

When  $|\hat{\sigma}^T \hat{\mathbf{b}}| \ll 1$ , the magnitude of the desired angular speed Eq. (8a) becomes very small, and the time needed to reach the equilibrium point grows. In this respect, it is possible to increase convergence speed dividing the original control law by a quantity which becomes vanishingly small, close to the equator, thus increasing the magnitude of the angular speed command. The modified

control law is given by

$$\boldsymbol{\omega}_d = -k_\tau \frac{(\hat{\boldsymbol{\tau}} - \hat{\boldsymbol{\sigma}}) \times \hat{\mathbf{b}}}{\hat{\mathbf{b}}^T \hat{\boldsymbol{\tau}} + \hat{\mathbf{b}}^T \hat{\boldsymbol{\sigma}}} \quad (15)$$

A formal proof by standard Lyapunov approach is not available, because the law in Eq. (15) is singular on the set  $\mathcal{E} = \partial\mathcal{A}$  and the sign of the angular velocity command switches across  $\mathcal{E}$ . Nevertheless, one can note that Eqs. (8a) and (15) differ only by a positive scalar quantity in  $\mathcal{A}$ , and a negative scalar in  $\mathcal{A}_\#$ , thus turning the point  $\hat{\boldsymbol{\sigma}} \equiv \hat{\boldsymbol{\sigma}}_\#$  into a globally attractive point on  $\mathcal{S}$  in the limit case  $\hat{\boldsymbol{\sigma}}^T \hat{\mathbf{b}} = 0$ .

#### IV. Results

A spacecraft model taken from [8] is considered for demonstrating the viability of the proposed approach, with an inertia tensor  $\mathbf{J} = \text{diag}(40.45, 41.36, 42.09) \text{ kg m}^2$ . The active reaction wheels have a moment of inertia  $J_w = 0.0077 \text{ kg m}^2$ . Values of the control gains,  $k_\omega = 0.1$  and  $k_\tau = 0.05$ , were selected by a trial-and-error procedure until a satisfactory convergence in terms of pointing error was obtained, without violating saturation limits on wheel rotation rate.

In the absence of privileged directions, a fixed target direction  $\hat{\boldsymbol{\tau}}_I = (1, 0, 0)^T$  in the inertial frame is assumed without lack of generality. Conversely, the position of the body-fixed axis  $\hat{\boldsymbol{\sigma}}$  that needs to be aligned with  $\hat{\boldsymbol{\tau}}$  has an influence on the response of the spacecraft, under the considered control law. In the ideal case, spacecraft and reaction wheels are assumed to be at rest at the initial time ( $\boldsymbol{\omega}_0 = 0$ ,  $\Omega_{i_0} = 0$ ), in order to satisfy the assumption of total angular momentum equal to zero during the maneuver. In order to test the control laws, Eqs. (8a) and (15), in a more realistic scenario, some cases were also run taking into account a non-zero residual angular momentum.

Figure 4 shows the simulation obtained using the nominal control law, for a (randomly specified) initial attitude, described by the quaternion  $\mathbf{q}_{BI} = (0.7792, 0.1225, -0.1051, 0.6056)^T$ , and a value of  $\lambda_\sigma = 30 \text{ deg}$ . The variation of RW spin rates (Fig. 4.a) proves that the control law determines a smooth response, while the pointing error  $\alpha$  and the non-nominal rotation angle  $\hat{\alpha}$  asymptotically converge towards zero, with an almost identical behavior and a convergence time in the order of approximately 150 s (Fig. 4.b). Maximum control torque, achieved at the beginning of the maneuver, is in the order of 0.2 N m. Peak values of control torques can be easily tailored by means of a proper

selection of control law gains

The nominal control law underperforms when  $\lambda_\sigma = 0$  and  $\hat{\sigma}$  is perpendicular to  $\hat{\mathbf{b}}$ . As shown in Fig. 5 by the solid line, the pointing error rapidly decreases from an initial value of 75 deg below 10 deg, before starting a very slow convergence towards zero. As many as 1200 s are necessary for taking the pointing error below a 1 deg threshold, because of the small value of the desired angular rate in the neighborhood of the desired direction. Conversely, the modified control law, Eq. (15) (dashed line), provides a faster convergence: 400 s are sufficient for achieving a pointing error below 0.01 deg, at the expenses of a higher initial command torque, increased by approximately 40% in the considered case.

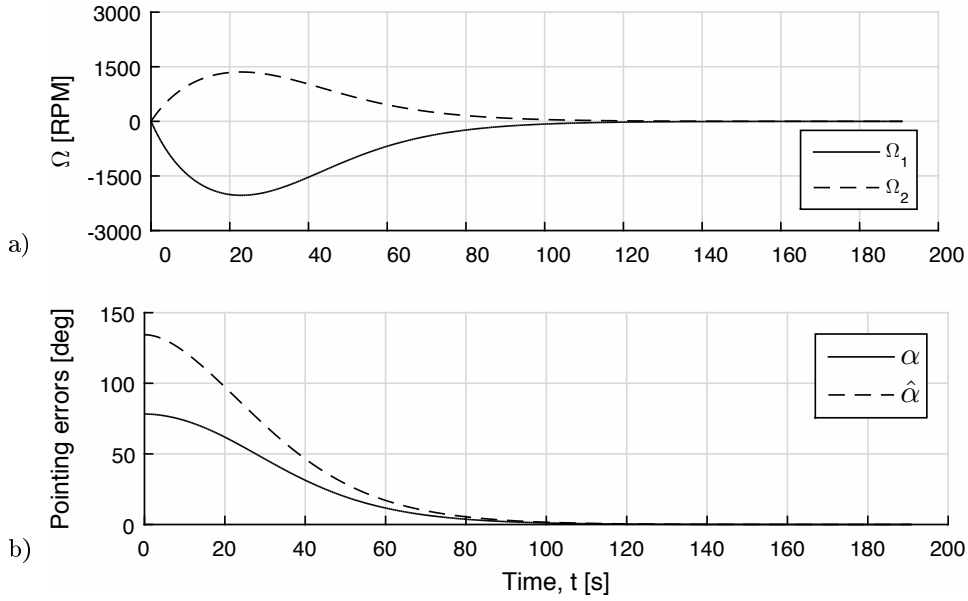


**Figure 4** Simulation results for  $\lambda_\sigma = 30$  deg and  $\mathbf{h} = \mathbf{0}$ : (a) wheel rates and (b) pointing errors for the nominal control laws ( $\alpha$ : angular distance;  $\hat{\alpha}$ : angular travel).

Robustness of the modified control law has been further verified through extensive numerical simulation, by means of a Monte Carlo analysis based on 250 cases featuring initial random attitude and random choice of  $\hat{\sigma}$ , for zero total angular momentum. Figure 6 shows the results of the analysis, where the logarithmic scale highlights an exponential decay of pointing error for all the tested cases.

Finally, the effects of relevant situations for real application are considered, namely (i) a misalignment between control axes and the principal axes of inertia and (ii) a small non-zero initial residual angular momentum, which takes into account that  $\mathbf{h}$  is brought close to zero during detum-

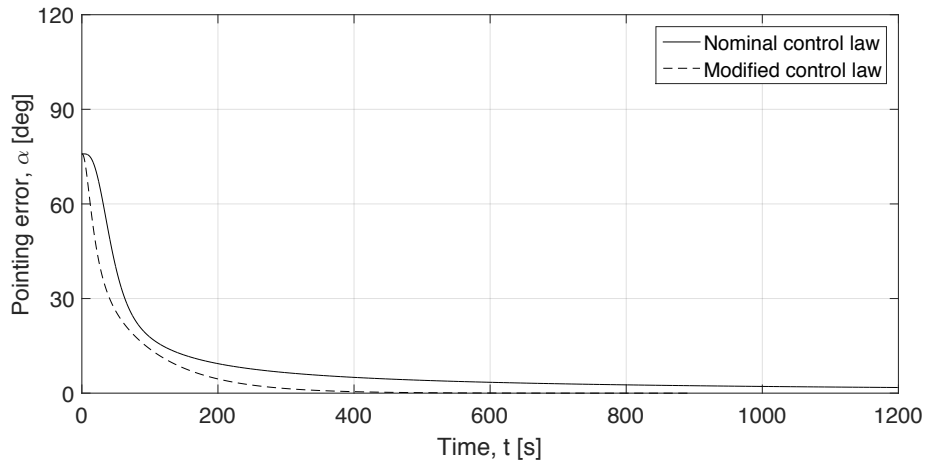


**Figure 5 Case  $\lambda_\sigma = 0$  deg with  $h = 0$ : pointing error  $\alpha$  for the nominal and modified control laws.**

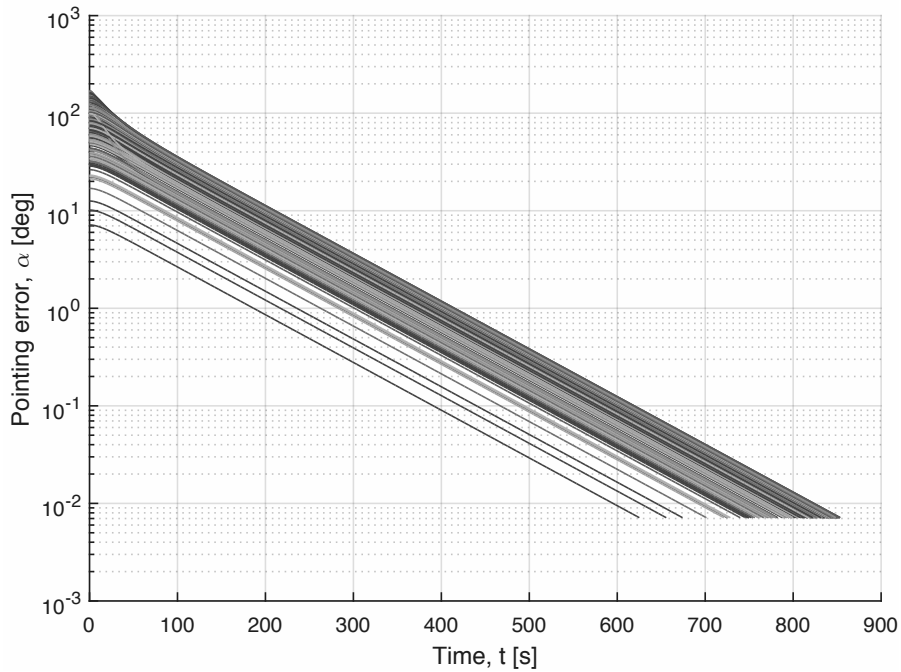


**Figure 6 Monte Carlo analysis: pointing error for the modified control law with  $h = 0$ .**

bling or desaturation phases (e.g. using magnetic actuators), but it cannot be exactly canceled. In the first case, the inertia tensor is not diagonal, but this fact has no practical effects on convergence. Results are not shown, provided there are only minor differences with respect to the time-histories already discussed for the nominal case.

As far as the single-axis pointing problem is concerned in the circumstance when  $h \neq 0$ , there

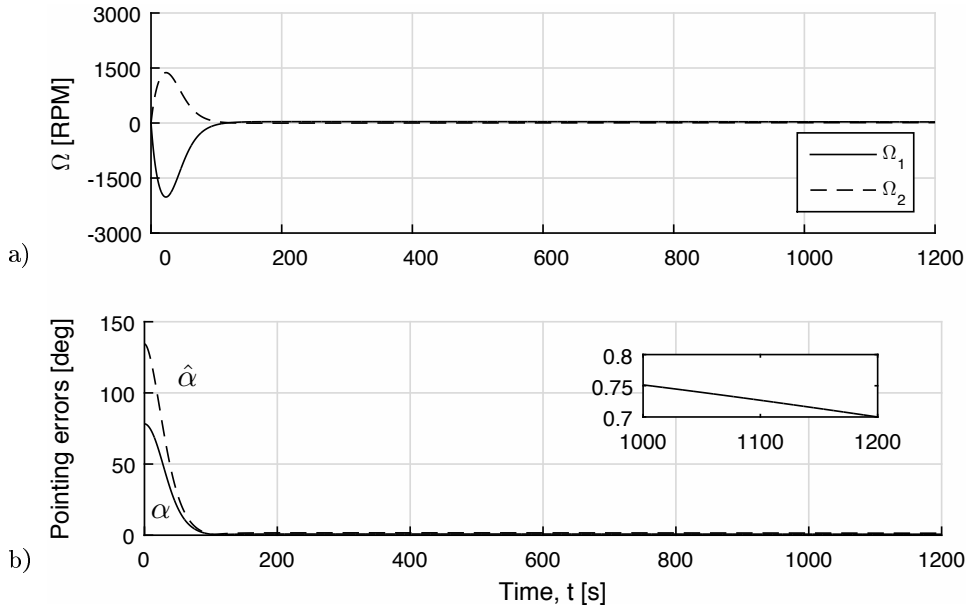


**Figure 7** Case  $\lambda_\sigma = 30$  deg with  $h = 0.01$  Nms: wheel rates and pointing errors for the nominal control law ( $\alpha$ : angular distance;  $\hat{\alpha}$ : angular travel).

is no apparent difficulty for the considered control law to exactly aim a body-fixed axis  $\hat{\sigma}$  towards a desired direction  $\hat{\tau}$ , if the residual angular momentum is sufficiently small, in the order between 0.001 and 0.01 Nms, for the considered class of spacecraft. Figure 7 shows that a steady-state pointing error in the order of few tenths of a degree is obtained for an initial value of  $h = (0.01, 0.01, 0.01)$  Nms, as in [8]. However, aligning an arbitrary (non-principal axes of inertia) body-axis  $\hat{\sigma}$  towards a given inertially-fixed direction may not be possible for higher values of  $h$ , when some regions of the attitude space become not accessible, if spacecraft rotation rates need to be driven to zero.

## V. Conclusions

The dynamic implementation of a kinematic planning strategy for single-axis pointing by means of two reaction wheels was demonstrated. An almost global stability to the desired alignment of a body-fixed axis towards an inertially-fixed direction was derived in the ideal conditions of zero total angular momentum, no reaction wheel torque saturation and wheel spin axis aligned with the principal axes of inertia.

The proposed control law generates an angular rate profile that tracks the desired rotation around an admissible rotation axis, that is, a rotation axis that lies on the plane of the two active

reaction wheels. This control law is smooth and almost global convergent for any considered case. As a minor drawback, slow convergence speed is obtained when the body-fixed axis to be pointed in the prescribed direction lies on the plane of the active RWs. To overcome this issue, a modified control law is also considered. Numerical simulation demonstrates the effectiveness of the proposed approach for any initial configuration and also in non-ideal conditions, that is, when a small residual angular momentum and a nondiagonal inertia tensor are considered.

### References

- [1] Roberts, B. A., Kruk, J. W., Ake, T. B., and Englar, T. S., “Three-axis Attitude Control with Two Reaction Wheels and Three-axis Attitude Control with Two Reaction Wheels and Magnetic Torquer Bars,” in “AIAA Guidance, Navigation, and Control Conference and Exhibit,” 2004-5245, 2004.
- [2] Duren, R. M., Dragon, K., Gunter, S. Z., Gautier, T. N., Bachtell, E., Peters, D. J., Harvey, A., Enos, A., Koch, D., Borucki, W., et al., “Systems engineering for the Kepler Mission: a search for terrestrial planets,” in “SPIE Astronomical Telescopes+ Instrumentation,” International Society for Optics and Photonics, 2004, pp. 16–27,  
doi:<http://dx.doi.org/10.1117/12.550276>.
- [3] “NASA Ends Attempts to Fully Recover Kepler Spacecraft, Potential New Missions Considered.” Last checked on April 22, 2016 on <http://www.nasa.gov/content/nasa-ends-attempts-to-fully-recover-kepler-spacecraft-potential-new-missions-considered/>5C%23.Vi3-oF53YTw, 2013.
- [4] Avanzini, G. and Giulietti, F., “Constrained Slews for Single-Axis Pointing,” *Journal of Guidance, Control, and Dynamics*, Vol. 31, No. 6, 2008, pp. 1813–1816,  
doi:<http://dx.doi.org/10.2514/1.38291>.
- [5] Tsiotras, P. and Longuski, J. M., “Spin-axis stabilization of symmetric spacecraft with two control torques,” *Systems & Control Letters*, Vol. 23, No. 6, 1994, pp. 395–402,  
doi:[http://dx.doi.org/10.1016/0167-6911\(94\)90093-0](http://dx.doi.org/10.1016/0167-6911(94)90093-0).
- [6] Kim, S. and Kim, Y., “Spin-Axis Stabilization of a Rigid Spacecraft Using Two Reaction Wheels,” *Journal of Guidance, Control, and Dynamics*, Vol. 24, No. 5, 2001, pp. 1046–1049,  
doi:<http://dx.doi.org/10.2514/2.4818>.
- [7] Tsiotras, P., Corless, M., and Longuski, M., “A Novel Approach to the Attitude Control of Axisymmetric Spacecraft,” *Automatica*, Vol. 31, No. 8, 1995, pp. 1099–1112,



doi:[http://dx.doi.org/10.1016/0005-1098\(95\)00010-T](http://dx.doi.org/10.1016/0005-1098(95)00010-T).

- [8] Horri, N. and Hodgart, S., "Attitude stabilization of an underactuated satellite using two wheels," in "Aerospace Conference, 2003. Proceedings. 2003 IEEE," Vol. 6, 2003, pp. 2629–2635,  
doi:<http://dx.doi.org/10.1109/AERO.2003.1235188>.
- [9] Horri, N. M. and Palmer, P., "Practical Implementation of Attitude-Control Algorithms for an Underactuated Satellite," *Journal of Guidance, Control, and Dynamics*, Vol. 35, No. 1, 2012, pp. 40–45,  
doi:<http://dx.doi.org/10.2514/1.54075>.
- [10] Yoon, H. and Tsiotras, P., "Spacecraft line-of-sight control using a single variable-speed control moment gyro," *Journal of Guidance, Control, and Dynamics*, Vol. 29, No. 6, 2006, p. 1295,  
doi:<http://dx.doi.org/10.2514/1.18777>.
- [11] Avanzini, G., de Angelis, E. L., and Giuliotti, F., "Single-Axis Pointing of Underactuated Spacecraft in the Presence of Path Constraints," *Journal of Guidance, Control, and Dynamics*, Vol. 38, No. 1, 2015, pp. 143–147,  
doi:<http://dx.doi.org/10.2514/1.G000121>.
- [12] Seibert, P. and Suarez, R., "Global stabilization of nonlinear cascade systems," *Systems & Control Letters*, Vol. 14, No. 4, 1990, pp. 347–352,  
doi:[http://dx.doi.org/10.1016/0167-6911\(90\)90056-Z](http://dx.doi.org/10.1016/0167-6911(90)90056-Z).
- [13] Khalil, H. K., *Nonlinear systems*, Prentice Hall, 2002. Pag. 125.